



Contents lists available at ScienceDirect

Journal of Biomechanics

journal homepage: www.elsevier.com/locate/jbiomech
www.JBiomech.com

Numerical modeling of bone tissue adaptation—A hierarchical approach for bone apparent density and trabecular structure

P.G. Coelho^a, P.R. Fernandes^{b,*}, H.C. Rodrigues^b, J.B. Cardoso^a, J.M. Guedes^b^a Mechanical and Industrial Engineering Department, FCT/UNL, Portugal^b IDMEC/IST, Technical University of Lisbon, Portugal

ARTICLE INFO

Article history:

Accepted 23 January 2009

Keywords:

Bone remodeling
Hierarchical
Bone surface
Anisotropy
Porosity

ABSTRACT

In this work, a three-dimensional model for bone remodeling is presented, taking into account the hierarchical structure of bone. The process of bone tissue adaptation is mathematically described with respect to functional demands, both mechanical and biological, to obtain the bone apparent density distribution (at the macroscale) and the trabecular structure (at the microscale). At global scale bone is assumed as a continuum material characterized by equivalent (homogenized) mechanical properties. At local scale a periodic cellular material model approaches bone trabecular anisotropy as well as bone surface area density. For each scale there is a material distribution problem governed by density-based design variables which at the global level can be identified with bone relative density. In order to show the potential of the model, a three-dimensional example of the proximal femur illustrates the distribution of bone apparent density as well as microstructural designs characterizing both anisotropy and bone surface area density. The bone apparent density numerical results show a good agreement with Dual-energy X-ray Absorptiometry (DXA) exams. The material symmetry distributions obtained are comparable to real bone microstructures depending on the local stress field. Furthermore, the compact bone porosity is modeled giving a transversal isotropic behavior close to the experimental data. Since, some computed microstructures have no permeability one concludes that bone tissue arrangement is not a simple stiffness maximization issue but biological factors also play an important role.

© 2009 Elsevier Ltd. All rights reserved.

1. Introduction

Bone remodeling is an enduring process that depends on biological and mechanical factors. Since, the statement of Wolff, generally called the Wolff's "Law" (Wolff, 1986), several mathematical and computational models for bone functional adaptation have been proposed (see e.g. Huiskes et al., 1987; Carter et al., 1987, 1989; Prendergast and Taylor, 1994; Martin, 1995; Jacobs et al., 1997; Hart and Fritton, 1997; Fernandes et al., 1999a; Doblaré and García, 2001, 2002). These models are of phenomenological nature, computing the change on bone apparent density (the result of osteoblasts and osteoclasts activity) for every point depending on a mechanical stimulus.

Some models consider bone as an isotropic structural material, which is a shortcoming on the treatment of trabecular bone, disregarding the importance of orientation in the remodeling process (Hart et al., 1984; Huiskes et al., 1987; Carter et al., 1987, 1989; Beaupré et al., 1990; Weinans et al., 1992). To overcome this, there are models that couple material density and orientation or

anisotropy (Jacobs et al., 1997; Hart and Fritton, 1997; Fernandes et al., 1999a; Rodrigues et al., 1999; Doblaré and García, 2001, 2002).

The present work extends the approach presented in two-dimensions by Rodrigues et al. (1999), i.e., it is a global–local hierarchical approach in which a global model of an entire bone supplies strain and density information to a series of local models characterizing the trabecular microstructure at each global model location. Bone is a hierarchical structural material, where several organizational levels can be identified from the macroscale to nanoscale (Lucchinetti, 2001). The two top levels corresponding to the entire bone and trabecular structure, respectively, show a suitable distribution of physical properties, such as bone density and corresponding mechanical properties, to achieve the functional requirements of bone tissue. Incorporating a material design scale in the remodeling model not only avoids any *a priori* assumption on material symmetries but also gives the possibility to take into account other trabecular architecture features such as bone surface area density. This additional step of going down one length-scale to model the microstructure adds the possibility of modeling actual biological features and approaches the phenomenological models to the biologically based models (mechanobiological), which try to consider both biological and mechanical

* Corresponding author. Tel.: +351 21 841 7925; fax: +351 21 841 7915.
E-mail address: prfernan@dem.ist.utl.pt (P.R. Fernandes).

factors based on bone cell activity (see e.g. Huiskes et al., 2000; Hazelwood et al., 2001; Hernandez, 2001; Hernandez et al., 2000; Taylor and Lee, 2003; Taylor et al., 2004; Garcia-Aznar et al., 2005).

In this work, the process of bone adaptation is described for two levels of the bone structure: the macroscopic level where the bone apparent density is determined and a microscopic level characterizing the trabecular structure. The law of bone remodeling is obtained assuming that bone adapts to functional demands in order to satisfy a multicriteria for structural stiffness and metabolic cost of bone formation. A three-dimensional example of the proximal femur subjected to physiological loading conditions is used to show the distribution of the apparent density, the anisotropic properties of internal trabecular architecture, the bone surface area density influence and the possibility of simulating/ diagnosing a disease scenarios of osteoporosis. In this work, porosity constraints are considered, affecting compact bone modeling. Finally, it is presented a validation of the hierarchical model based on Dual-energy X-ray Absorptiometry (DXA) results.

2. Materials and methods

2.1. Material model

The hierarchical bone remodeling model assumes bone as a porous (cellular) periodic material. The material model comprises two scales to characterize bone tissue as shown in Fig. 1. At macroscale a design domain Ω corresponds to the whole bone domain subjected to surface tractions \mathbf{t} along Γ_t and imposed displacements \mathbf{u} along Γ_u . At microscale a design domain Y is defined as being the trabecular scale. The model computes not only a relative (apparent) density ρ in each point \mathbf{x} of Ω but also a volume fraction μ in each point \mathbf{y} of Y . Therefore, a two-scale material distribution problem (macro and micro) can be identified and the density-based design variables govern each scale, $\rho(\mathbf{x})$ and $\mu(\mathbf{x}, \mathbf{y})$, respectively.

At each point \mathbf{x} in Ω the bone relative density ρ lies in the interval $]0, \rho_{\max}]$, where $\rho_{\max} \leq 1$, and the limits identify bone absence (white) and compact bone (black), respectively. An intermediate value of ρ (gray) means the existence of a porous material at microscale (spongy bone) that is characterized by the geometry of a single (unit) cell assumed periodically repeated inside a small neighborhood of a point $\mathbf{x} \in \Omega$. Such a geometry is the solution of the local problem in Y where $\mu \in]0, 1]$. The base material within the unit cell is assumed linear and isotropic. The macro-density ρ is coupled with micro-density μ through

$$\rho(\mathbf{x}) = \frac{1}{|Y|} \int_Y \mu(\mathbf{x}, \mathbf{y}) dY, \quad \forall \mathbf{x} \in \Omega \quad (1)$$

2.2. Law of bone remodeling

The law of bone remodeling assumes that bone adapts to functional demands in order to satisfy a multicriteria for structural stiffness (maximized) and metabolic cost k of bone formation (minimized) that depends on biological factors such as: disease, hormonal status, age or sex. Since, the time scale of applied force change is much smaller than the bone remodeling time scale one characterizes the applied forces as a weighted set of P loads characterizing the loading environment applied to bone. For these criteria, the bone adaptation is modeled as a two-scale optimization problem formulated in the following way (see also Rodrigues et al., 1999 and Coelho et al., 2008 for full optimization model description):

$$\min_{\substack{\rho(\mathbf{x}) \\ \rho_{\min} \leq \rho(\mathbf{x}) \leq \rho_{\max}}} F(\rho) \quad \text{with } F(\rho) = \int_{\Omega} \Phi(\rho, \mathbf{u}^1, \dots, \mathbf{u}^P) d\Omega + k \left(\int_{\Omega} \rho(\mathbf{x}) d\Omega \right) \quad (2)$$

$$\Phi(\rho, \mathbf{u}^1, \dots, \mathbf{u}^P) = \max_{\substack{\mu(\mathbf{y}) \\ \rho_{\min} \leq \rho(\mathbf{x}) \leq \rho_{\max} \\ \int_Y \mu(\mathbf{y}) dY = \rho(\mathbf{x})}} f(\mu) \quad \text{where } f(\mu) = \sum_{r=1}^P \alpha^r \left[\frac{1}{2} E_{ijkl}^H(\mu) \varepsilon_{ij}(\mathbf{u}^r) \varepsilon_{kl}(\mathbf{u}^r) \right] \quad (3)$$

where $\varepsilon(\mathbf{u})^r$ is the strain tensor for the displacement field \mathbf{u}^r solution of the equilibrium equation for the global problem and the r^{th} load, and E_{ijkl}^H are the homogenized properties for the trabecular bone at point $\mathbf{x} \in \Omega$ (see Guedes and Kikuchi, 1990). The parameter α^r is the weight for the r^{th} load case characterizing its relative importance and $\sum_{r=1}^P \alpha^r = 1$.

The stationarity of multiscale optimization problem (2) and (3) with $\rho_{\max} = 1$ leads to the remodeling rate equation

$$\frac{d\mu}{dt} = \frac{\partial E_{ijkl}^H(\mu)}{\partial \mu(\mathbf{x}, \mathbf{y})} \sum_{r=1}^P [\alpha^r \varepsilon_{ij}(\mathbf{u}^r) \varepsilon_{kl}(\mathbf{u}^r)] - k \quad (4)$$

which gives the change on micro-density with time t (steps of the optimization algorithm) until the remodeling equilibrium is achieved, i.e., until the following equation is satisfied

$$\frac{\partial E_{ijkl}^H(\mu)}{\partial \mu(\mathbf{x}, \mathbf{y})} \sum_{r=1}^P [\alpha^r \varepsilon_{ij}(\mathbf{u}^r) \varepsilon_{kl}(\mathbf{u}^r)] - k = 0 \Rightarrow \frac{d\mu}{dt} = 0 \quad (5)$$

Thus, at the cellular material level (“microstructure”), and assuming the multiload formulation, the rate equation characterizing the material volume fraction evolution with time is of the following type:

$$\frac{d\mu}{dt} = B(\mu)_{ijkl} \sum_{r=1}^P [\alpha^r \varepsilon_{ij}^r \varepsilon_{kl}^r] + C(\mu) \quad (6)$$

This type of remodeling law can also be understood as a generalization of several bone remodeling models using strain energy density as stimulus (see e.g. Mullender et al., 1994), where evolution coefficients $B(\mu)$ and $C(\mu)$ are obtained by the solution of the problem (2) and (3).

Compact bone is neither fully dense nor isotropic, it is a porous medium with 5–10% of porosity and usually considered transversally isotropic (Martin et al., 1998). In order to better approach real compact bone microstructure (specially the

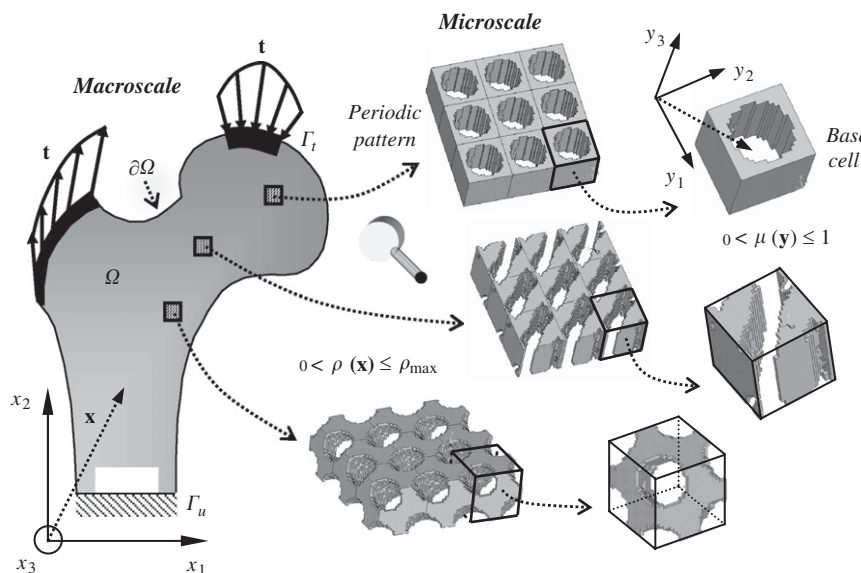


Fig. 1. Two-level bone remodeling model.

modeling of vascular porosity, see Cowin, 1999), a minimum level of porosity can be ensured by the proposed model decreasing the upper bound of the apparent bone density in Eq. (2), i.e., $\rho_{\max} < 1$. This restriction as well as the introduction of specific features on microstructures design needs an efficient algorithmic strategy to solve Eqs. (2) and (3). The strategy used here combines two optimizers, taking each one the respective density-based design variable, ρ or μ . Fig. 2 shows the flowchart describing the running of the algorithm. The two-scale model (see Fig. 1 and Eqs. (2) and (3)) implies the iterative solution of one problem at a global (or macro) scale to find ρ (outer loop) and several problems at a local (or micro) scale (inner loop) to characterize the material microstructure variable μ . Here, the Method of Moving Asymptotes—MMA (see Svanberg, 1987) to solve Eq. (2) and find ρ is combined with CONVex LINearization—CONLIN (see Fleury 1989) to solve (3) and obtain μ . This strategy is quite appropriate to deal with criteria and constraints that should be considered at the microstructure level, and thus takes full advantage of the hierarchical formulation. Next section discusses the introduction into the micro-problem of this type of criterion namely a biologically driven constraint present in trabecular bone.

2.3. Bone surface area density

A morphometric parameter characterizing trabecular architecture is the surface-to-volume ratio known as “bone surface area density”, S_v (see Beaupré et al., 1990). Several authors have studied this surface-to-volume ratio for both bone samples and bone idealized microstructure models and concluded that a strong relationship exists between S_v and apparent density or volume fraction ρ (see e.g. Parfitt et al., 1983; Martin, 1984; Fazzalari et al., 1989; Fyhrie et al., 1993; Fyhrie et al., 1995). The resulting curves plotted in Fig. 8a illustrate that the bone surface area available for remodeling is not a uniform function of density but rather has a maximum at bone intermediate volume fraction values. Thus, substantial differences in the potential rate of bone loss or gain exist for bone regions with different apparent densities (Beaupré et al., 1990).

The hierarchical approach allows the application of a surface measure to the microstructure design and thus introduces the bone surface as a biologically driven condition for bone adaptation.

The internal microstructure surface is measured through the generalized area measure function $g(\mu)$ based on the total variation of the micro-density field, μ , and given by

$$g(\mu) = \int_{\Gamma_j} \left[\left(\langle \mu \rangle^2 + \varepsilon^2 \right)^{1/2} - \varepsilon \right] d\Gamma_i \quad (7)$$

In Eq. (7), $\langle \mu \rangle$ is the jump on the material volume fraction function, Γ_j is the respective discontinuity boundary (each finite element boundary in the numerical model) and ε stands for differentiability (for a detailed description see Bendsoe and Sigmund, 2003; Fernandes et al., 1999b).

In terms of mathematical formulation, problem (3) considers now an additional constraint for minimum surface area density

$$\left(\frac{\beta}{|Y|} \right) g(\mu) \geq S_v^* \quad \text{where,} \quad S_v^* = -0.2412 + 24.8\rho - 64.7\rho^2 + 103.7\rho^3 - 67.5\rho^4 \quad (8)$$

In Eq. (8), $|Y|$ is the cell volume taken as $1.5 \times 1.5 \times 1.5 \text{ mm}^3$ to accommodate a mean pore diameter varying from 300 to 1500 μm (Keaveny et al., 2001). The parameter β is selected to correct the surface overestimation due to the presence of intermediate densities in the microstructure definition (β is set to $\frac{2}{3}$). The surface area density function S_v^* , used in Eq. (8) is chosen as a compromise among the data reported by several authors (see bold curve in Fig. 8a).

3. Results

3.1. Proximal femur

The hierarchical model is evaluated in a finite element approximation of a proximal left human femur. The bone geometry is based on the standardized femur (Viceconti et al., 1996). The femur bone domain Ω and cell domain Y are discretized by 2112 and 8000 ($20 \times 20 \times 20$) hexahedral isoparametric finite elements of 8 nodes, respectively. Within the respective finite element Ω^E and Y^e the densities ρ and μ are assumed to be constant. The initial spatial distribution of macro- and micro-densities is homogeneous and non-homogeneous, respectively (see Coelho et al., 2008). The results correspond to a global bone mass of 50%, i.e., $k = 1050$ in Eq. (2).

The multiload case considered here is based on the data reported in (Bergmann, 1998; Bergmann et al., 2001). Ten load cases were considered ($P = 10$). A first set of five load cases corresponds to normal walking activity and a second one

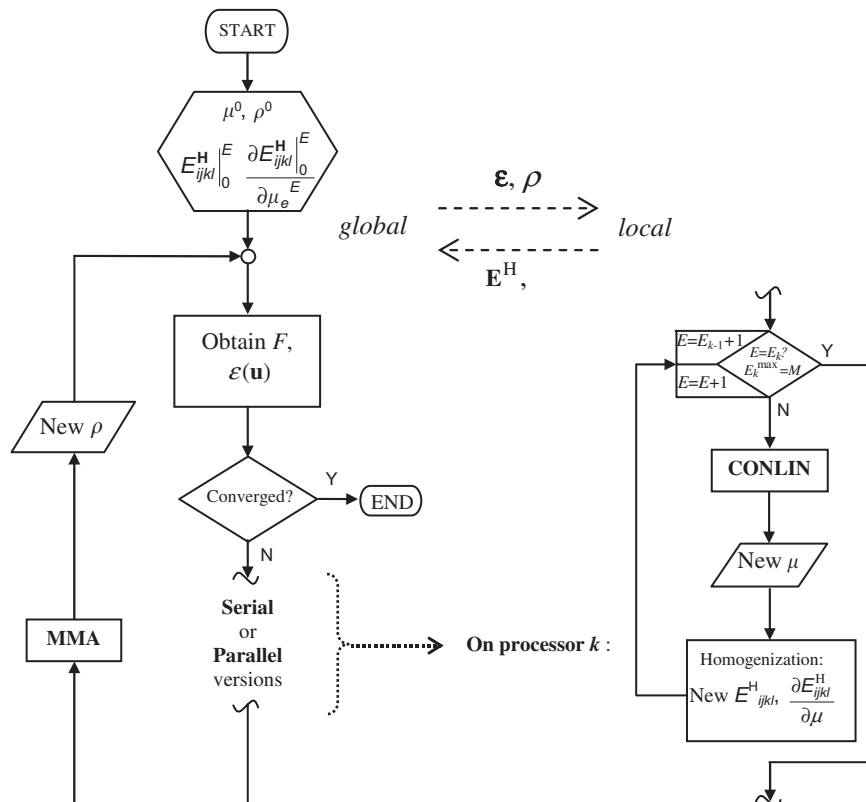


Fig. 2. Flowchart for the MMA/CONLIN algorithmic strategy (highlighted the parallel version).

corresponds to stair climbing. All load cases have equal importance, $\alpha = 0.1$ in Eq. (3).

The interpolation scheme between material properties and micro-density is Solid Isotropic Model with Penalization (SIMP) with an exponent equal to 4 (see Coelho et al., 2008 for details). It is assumed to be an isotropic base material defined by 20 GPa of Young's modulus and 0.3 of Poisson's ratio. It should be remarked that the base material properties correspond to the properties of mineralized bone tissue. The true density of the mineralized tissue is approximately constant in all trabecular and cortical bone (Carter and Beaupré, 2001). Thus, trabecular bone is made by a combination of dense mineralized struts and pores, while compact bone is a mineralized matrix crossed by canals ("haversian canals"). Once a micro-density distribution is known,

the bone equivalent properties, both for trabecular and compact bone, are obtained by homogenization, taking into account the microstructural arrangement of each type of bone.

The obtained apparent density distribution, shown in Fig. 3, reproduces some characteristics of the real femur such as: the external compact bone layer (black), the medullar cavity and the less dense spongy bone in the femoral head, with the Ward's triangle clearly identified. Fig. 4 shows the obtained microstructures corresponding to different anatomic regions. The microstructures identified as 1, 2 and 3 correspond to cortical bone located at lateral and medial midshaft. The cortical bone is not modeled here as a local full material solution (isotropic) but instead as a porous medium matching real bone porosity (5–10%, see Martin et al., 1998). A value of 7.5% has been used in this example, i.e., $\rho_{\max} = 0.925$ in (2). As shown in Fig. 5, the porosity constraint $\rho_{\max} = 0.925$ results on voids (longitudinal tunnels) resembling Haversian canals, which are actually the main contribution for cortical bone porosity and anisotropy (transversal isotropy). In Fig. 5 the plot for the anisotropy (component $1/C_{1111}^H$ of the compliance tensor is plotted in all directions of the space) shows a transverse isotropic behavior although the ratio between longitudinal and transversal elastic modulus is about 1.3, slightly lower than the experimental data (≈ 1.5 , see Lucas et al., 1999).

The cellular material solutions in Fig. 4 are more or less dense/anisotropic depending on anatomic region and respective stress fields. In regions where a triaxial state of stress is dominant the microstructures are equiaxed (closest to isotropic behavior). There are regions where microstructures are strongly oriented. For uniaxial stress field and biaxial the resulting microstructures become like honeycomb or parallel plates structures, respectively. In these regions the mechanical behavior is anisotropic. These results agree with idealized bone microstructures as presented by several authors (see e.g. Gibson and Ashby, 1988).

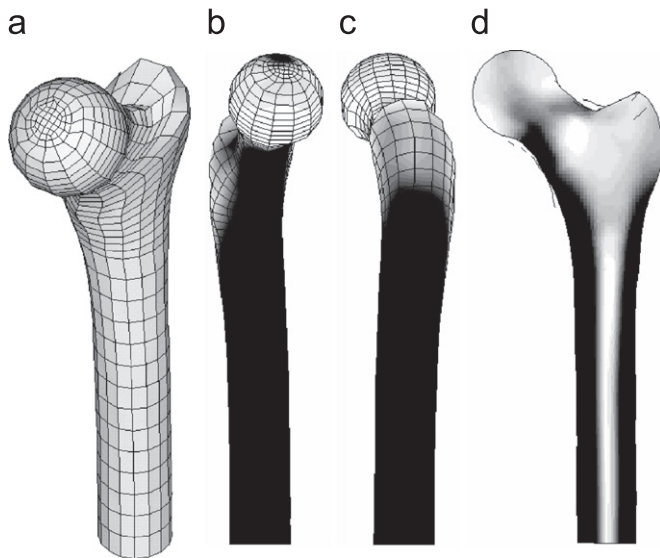


Fig. 3. (a) Global finite element mesh (left femur); apparent density distribution without surface control (average of nodal values); (b) medial-lateral view; (c) lateral-medial view; (d) coronal middle sectional view.

3.2. Bone surface area influence

In this section the numerical results with surface control (problem (3) has an extra constraint as described in Section 2.3)

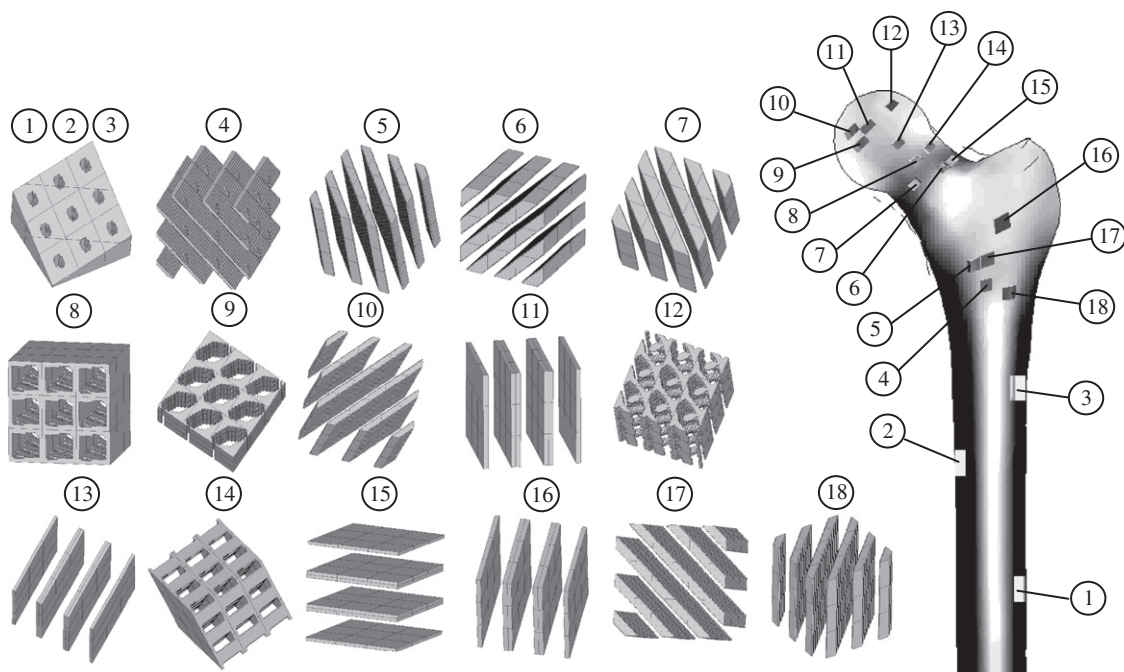


Fig. 4. Several microstructures depending on anatomic site (without surface control).

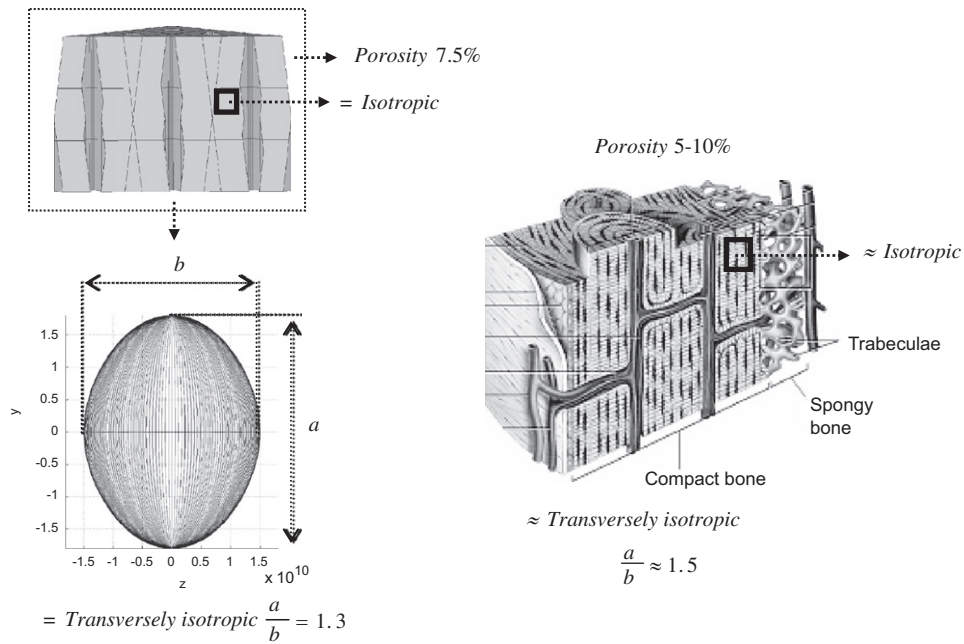


Fig. 5. Orthotropy of compact bone. Numerical results on left. Experimental data on right.

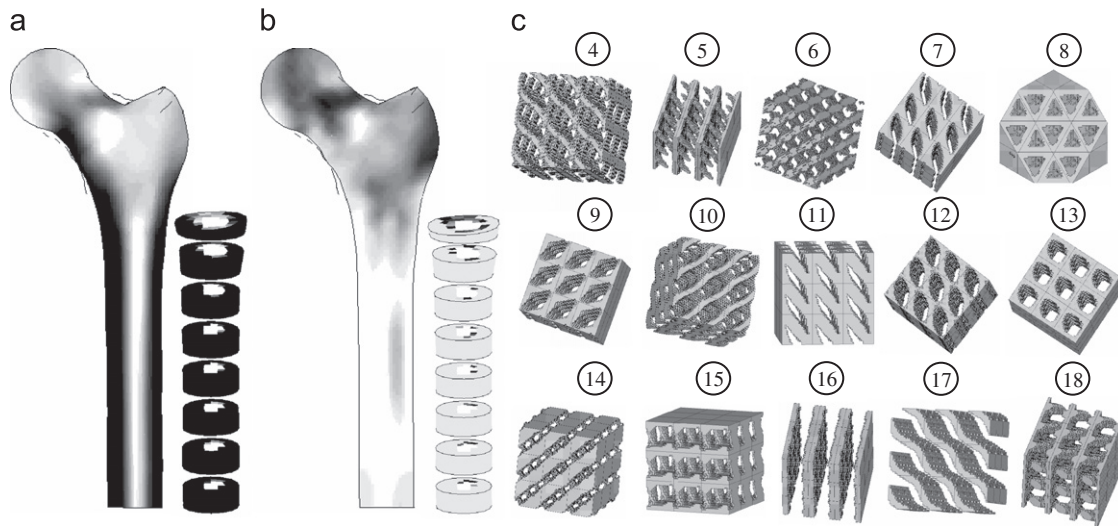


Fig. 6. Results with surface control. Coronal middle sectional view and 3D view of diaphysis: (a) apparent density distribution; (b) surface distribution. (c) microstructures numbered as in Fig. 4.

are compared with those without surface control shown in Section 3.1. At macroscale the differences on density distribution with and without surface control seem insignificant when comparing Figs. 3d and 6a. Furthermore, Fig. 6b shows how surface is distributed over the global domain (cross-sectional view) identifying femur's head as the region with higher surface values, agreeing with reality, since trabecular bone has a higher surface-to-volume ratio.

At the microscale the effect of surface control is more notorious when observing the results (see Fig. 6c). These results should be compared with those of Fig. 4 where the microstructures obtained without surface control and for the same macroelements are shown. Basically, from this comparison it is clear that when surface control is active the microstructures have a higher surface area and are closer to real bone architecture. In general, without surface control micro-solutions tend to exhibit a

lack of connectivity (case of laminates) whereas if the surface is prescribed the material cell interconnectivity improves.

The Fig. 7 highlights the influence of surface control on the volume fraction distribution. From this plot one can observe that when surface control is active the distribution is more regular. Furthermore, the distribution of volume fraction values is physiologically more consistent. There is a gap in the volume fractions between 0.5 and 0.9 i.e., the transition from trabecular to cortical bone is abrupt, reproducing a biological reality.

Also, with surface control, the numerically obtained bone surface area density retrieves the analytical function S^* , given in (8), (see Fig. 8a and b). This means that the resulting microstructures maximize stiffness while exhibiting a proper surface-to-volume ratio consistent with biological mechanisms involving bone cells activity.

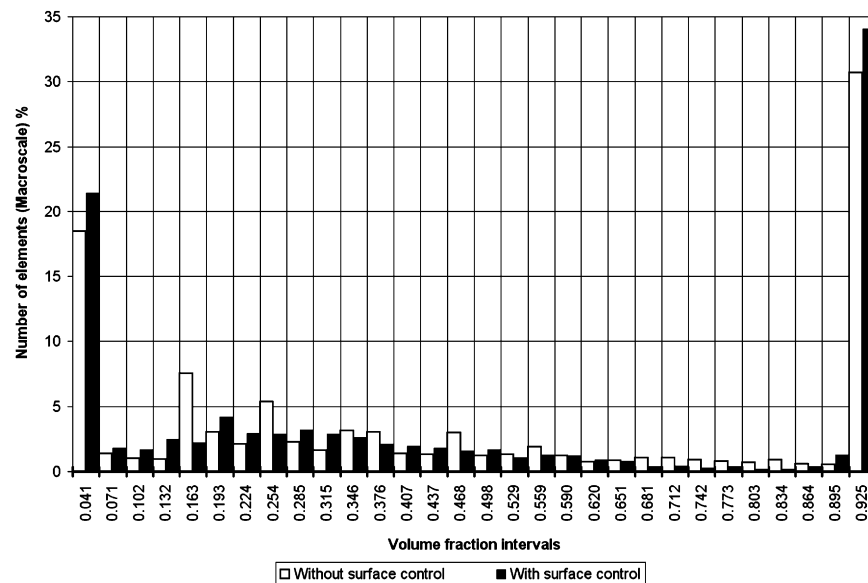


Fig. 7. Counting the number of macro-finite elements (%) in existence within each interval of volume fraction.

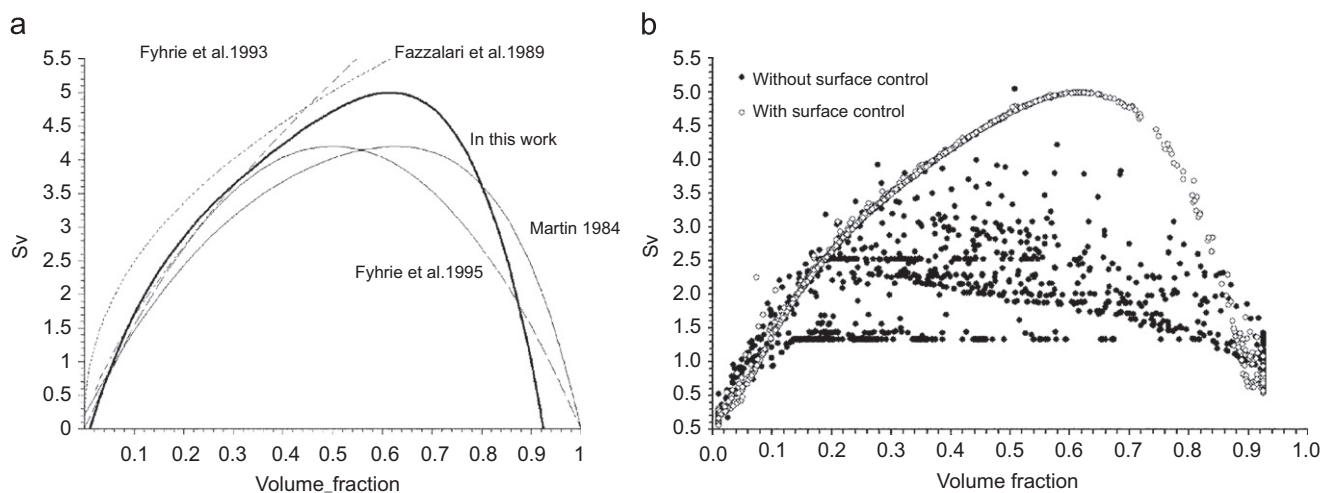


Fig. 8. Plotting bone surface area density [mm^2/mm^3] as a function of volume fraction: (a) curves from the literature and the one used in this work (in bold); (b) numerical results with and without surface control.

The Fig. 8b also allows inferring about the optimality of bone structure. When surface is not controlled a cluster of points is obtained typically below the reference curve S_v^* , which suggests once again that bone is not simply optimized for stiffness. Even though scattered over an area, these points seem to form characteristic curves. This distribution trend may be compared with some analytical models for trabecular bone assuming simpler microstructures for trabecular bone characterization (rod, plate, plate and rod, 3D rod, spherical hole, see e.g. Fazzalari et al., 1989). For instance, the points falling in the plateau with $S_v = 1.333$ (see Fig. 8b) correspond to a plate-like model for bone. However, bone architecture does not show simply parallel plates, in fact they are “perforated plates” linked through small “bars”.

3.3. Effect of metabolic cost parameter

The results from *Dual-energy X-ray Absorptiometry* exams in Fig. 9a show how healthy bone may degenerate due to a disease scenario (osteoporosis). These changes on bone may be simulated

through the parameter k in Eq. (2). As k increases the total amount of bone mass decreases as shown in Fig. 9b (note that here, “white” is compact bone and “black” bone absence for direct comparison with DXA images). Santos et al. (2008) shows that a correlation can be mathematically established between k and T -score results from *Dual-energy X-ray Absorptiometry* exams (for further details see Santos et al., 2008). This quantitative correlation is used to qualitatively validate the hierarchical model results through the comparison between Fig. 9a and b. The DXA exam shown in Fig. 9a (top) was chosen from a T -score that is mathematically correlated with the k value equal to 550 (see Fig. 9b). Likewise, the DXA image Fig. 9a (bottom) is correlated with k equal to 3100 (see Fig. 9b).

Fig. 10 shows four bone microstructures and their evolution when k increases. These results reproduce some physiological events in an osteoporotic evolution at trabecular level. Initially, bone loss leads to trabeculae thinning with no loss of connectivity. When bone loss becomes severe, the trabeculae thinning process degenerates on loss of connectivity, which actually has a major effect on bone strength and increases the risk of fracture.

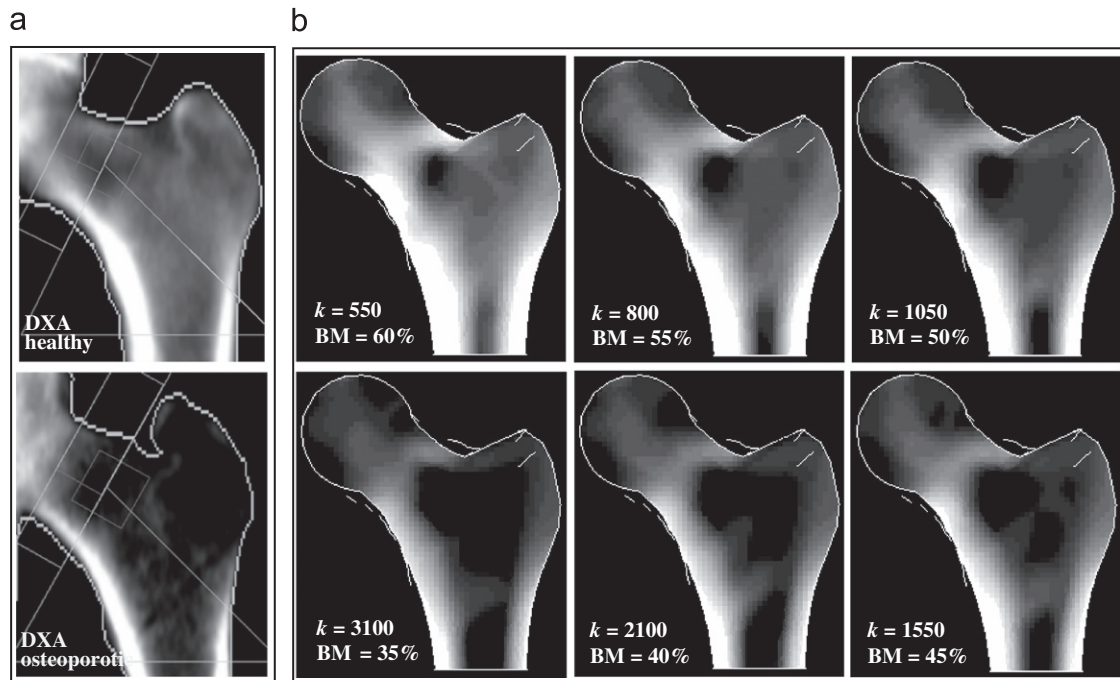


Fig. 9. Qualitative comparison between DXA exams and numerical results obtained varying k : (a) on top DXA showing healthy bone (compares with $k = 550$) and on bottom DXA result showing osteoporotic bone (compares with $k = 3100$); (b) numerical results of bone apparent density in terms of metabolic cost parameter k (bone mass BM in % and coronal middle sectional view).

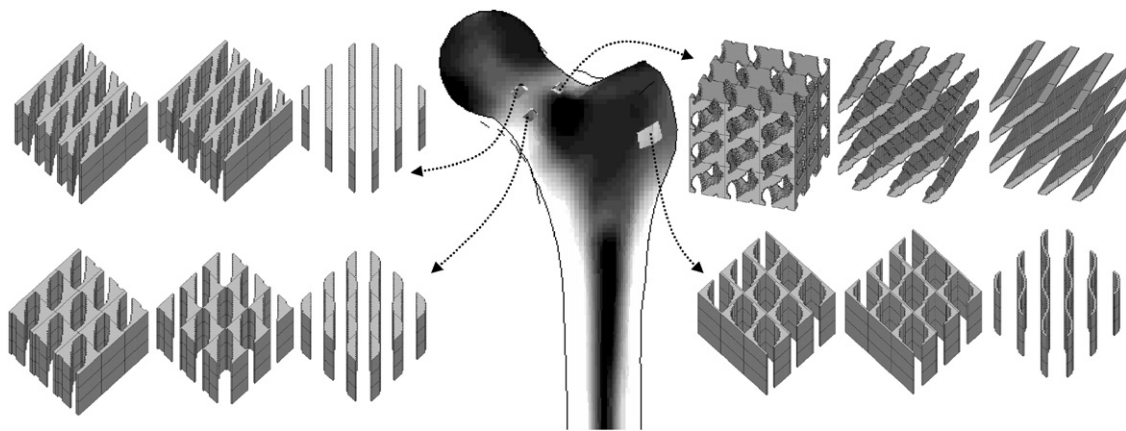


Fig. 10. Microstructure evolution for k increase (from left to right in each element).

4. Conclusion

A three-dimensional hierarchical model for bone tissue adaptation is presented allowing for the introduction of constraint at the micro-level. The model is able to provide an apparent density distribution that fairly approximates the real femur bone at macroscale. At microscale the obtained microstructures characterize the local microstructure of compact and trabecular bone with the respective anisotropic properties.

The compact bone was modeled with a porosity constraint and the numerical results agree with the transversely isotropic behavior, as measured experimentally. Concerning the resulting microstructures modeling trabecular bone, the present model allows the introduction of specific bone features such as bone surface area density.

The hierarchical model gives an understanding on bone loss scenarios, either at macroscale or at trabecular (micro) scale. This

is possible through the variation of the parameter related to the metabolic cost of bone formation. A strong correlation between this parameter and T -score (DXA) results can be found, allowing the qualitative validation of the model. Since imaging tools like DXA have limitations, in the assessment of bone quality *in vivo*, the validated numerical remodeling models may play an important role as fracture-risk predictive tools.

Some microstructures modeling regions of trabecular bone, present closed walls, i.e., they do not satisfy the porosity/permeability property encountered in real bone. Since porosity/permeability is critical for biological requirements, such as cell migration and vascularization, one concludes that mechanisms more complex than simple stiffness optimization play an important role in trabecular bone architecture (see also Sigmund, 1999).

This model represents a new approach to computational prediction of bone adaptation, both for apparent density and

trabecular architecture mechanical behavior. Thus, it can be a valuable tool to medical diagnoses, to gain insight into the fine structure of bone, namely on osteoporosis, as well as to support scaffolds design in tissue engineering.

Conflict of interest statement

There is not any financial and personal relationship with other people or organizations that could inappropriately influence this work.

Acknowledgements

This work was supported by the FCT through the Project PTDC/EME-PME/71436/2006 and PhD scholarship—SFRH/BD/25033/2005 (P. Coelho). The results presented here were produced using the IST Cluster (IST/Portugal). We would like to thank Doctor João Eurico Fonseca (Rheumatology and Metabolic Bone Disease Department in Sta. Maria Hospital, Lisbon, Portugal) for the DXA analysis images and professor Krister Svanberg (Royal Institute of Technology, Stockholm, Sweden) for the MMA codes.

References

- Bendsøe, M.P., Sigmund, O., 2003. *Topology Optimization Theory, Methods and Applications*. Springer, Berlin Heidelberg, New York.
- Beaupré, G.S., Orr, T.E., Carter, D.R., 1990. An approach for time-dependent bone modeling and remodeling-theoretical development. *Journal of Orthopaedic Research* 8, 651–661.
- Bergmann, G., 1998. Hip98—Loading of the hip joint. Free University of Berlin. Compact disc, ISBN 3980784800.
- Bergmann, G., Deuretzbacher, G., Heller, M., Graichen, F., Rohlmann, A., Strauss, J., Duda, G., 2001. Hip contact forces and gait patterns from routine activities. *Journal of Biomechanics* 34, 859–871.
- Carter, D.R., Beaupré, G.S., 2001. *Skeletal Function and Form*. Cambridge University Press.
- Carter, D.R., Fyhrie, D.P., Whalen, R.T., 1987. Trabecular bone density and loading history: regulation of tissue biology by mechanical energy. *Journal of Biomechanics* 20, 785–795.
- Carter, D.R., Orr, T.E., Fyhrie, D.P., 1989. Relationships between loading history and femoral cancellous bone architecture. *Journal of Biomechanics* 22, 231–244.
- Coelho, P., Fernandes, P., Guedes, J., Rodrigues, H., 2008. A hierarchical model for concurrent material and topology optimization of three-dimensional structures. *Structural and Multidisciplinary Optimization* 35, 107–115.
- Cowin, S.C., 1999. Bone poroelasticity. *Journal of Biomechanics* 32, 217–238.
- Doblaré, M., Garcia, J.M., 2001. Application of an anisotropic bone-remodelling model based on a damage-repair theory to the analysis of the proximal femur before and after total hip replacement. *Journal of Biomechanics* 34, 1157–1170.
- Doblaré, M., Garcia, J.M., 2002. Anisotropic bone remodelling model based on a continuum damage-repair theory. *Journal of Biomechanics* 35, 1–17.
- Fazzalari, N.L., Crisp, D.J., Vernon-Roberts, B., 1989. Mathematical modeling of trabecular bone structure: the evaluation of analytical and quantified surface to volume relationships in the femoral head and iliac crest. *Journal of Biomechanics* 22, 901–910.
- Fernandes, P., Rodrigues, H., Jacobs, C., 1999a. A model of bone adaptation using a global optimization criterion based on the trajectorial theory of Wolff. *Computer Methods in Biomechanics and Biomedical Engineering* 2, 125–138.
- Fernandes, P., Guedes, J.M., Rodrigues, H., 1999b. Topology optimization of three-dimensional structures with a constraint on perimeter. *Computers and Structures* 73, 583–594.
- Flury, C., 1989. CONLIN: an efficient dual optimizer based on convex approximation concepts. *Structural Optimization* 1, 81–89.
- Fyhrie, D.P., Fazzalari, N.L., Goulet, R., Goldstein, S.A., 1993. Direct calculation of the surface-to-volume ratio for human cancellous bone. *Journal of Biomechanics* 26, 955–967.
- Fyhrie, D.P., Lang, S.M., Hoshaw, S.J., Shaffler, M.B., Kuo, R.F., 1995. Human vertebral cancellous bone surface distribution. *Bone* 17, 287–291.
- Garcia-Aznar, J.M., Rueberg, T., Doblaré, M., 2005. A bone remodelling model coupling microdamage growth and repair by 3D BMU-activity. *Biomechanics and Modeling Mechanobiology* 4, 147–167.
- Gibson, L., Ashby, M., 1988. *Cellular Solids, Structure and Properties*. Pergamon Press, Oxford, England.
- Guedes, J., Kikuchi, N., 1990. Preprocessing and postprocessing for materials based on the homogenisation method with adaptive finite element method. *Computer Methods in Applied Mechanics and Engineering* 83, 143–198.
- Hart, R.T., Davy, D.T., Heiple, K.G., 1984. A computational model for stress analysis of adaptive elastic materials with a view toward applications in strain-induced bone remodeling. *Journal of Biomechanical Engineering* 106, 342–350.
- Hart, R.T., Fritton, S.P., 1997. Introduction to finite element based simulation of functional adaptation of cancellous bone. *Forma* 12, 277–299.
- Hazelwood, S.J., Martin, R.B., Rashid, M.M., Rodrigo, J.J., 2001. A mechanistic model for internal bone remodeling exhibits different dynamic responses in disuse and overload. *Journal of Biomechanics* 34, 299–308.
- Hernandez, C.J., Beaupré, G.S., Carter, D.R., 2000. A model of mechanobiologic and metabolic influences on bone adaptation. *Journal Rehabilitation Research and Development* 37, 235–244.
- Hernandez, C.J., 2001. Simulation of bone remodeling during the development and treatment of osteoporosis. PhD thesis, Stanford University, Stanford, CA.
- Huiskes, R., Weinans, H., Grootenboer, H.J., Dalstra, M., Fudala, B., Sloof, T.J., 1987. Adaptive bone-remodeling theory applied to prosthetic-design analysis. *Journal of Biomechanics* 20, 1135–1150.
- Huiskes, R., Ruimerman, R., van Lenthe, G.H., Janssen, J.D., 2000. Effects of mechanical forces on maintenance and adaptation of form in trabecular bone. *Nature* 405, 704–706.
- Jacobs, C.R., Simo, J.C., Beaupré, G.S., Carter, D.R., 1997. Adaptive bone remodeling incorporating simultaneous density and anisotropy considerations. *Journal of Biomechanics* 30, 603–613.
- Keaveny, T.M., Morgan, E.F., Niebur, G.L., Yeh, O.C., 2001. Biomechanics of trabecular bone. *Annual Review of Biomedical Engineering* 3, 307–333.
- Lucas, G., Cook, F., Friis, E., 1999. *A Primer of Biomechanics*. Springer, NY.
- Lucchinetti, E., 2001. Composite model of bone properties. In: Cowin, S.C. (Ed.), *Bone Mechanics Handbook*, 2nd Edition. CRC Press, pp. 121–1219.
- Martin, R.B., 1984. Porosity and specific surface of bone. *CRC Critical Reviews in Biomedical Engineering* 10, 179–222.
- Martin, R.B., 1995. A mathematical model for fatigue damage repair and stress fracture in osteonal bone. *Journal Orthopaedic Research* 13, 309–316.
- Martin, R.B., Burr, D.B., Sharkey, N.A., 1998. *Skeletal Tissue Mechanics*. Springer, NY.
- Mullender, M.G., Huiskes, R., Weinans, H., 1994. A Physiological approach to the simulation of bone remodeling as a self-organisational control process. *Journal of Biomechanics* 27, 1389–1394.
- Parfitt, A.M., Mathews, C.H., Villanueva, A.R., Kleerekoper, M., Frame, B., Rao, D.S., 1983. Relationships between surface, volume, and thickness of iliac trabecular bone in aging and in osteoporosis. *Journal Clinical Investigation* 72, 1396–1409.
- Prendergast, P.J., Taylor, D., 1994. Prediction of bone adaptation using damage accumulation. *Journal of Biomechanics* 27, 1067–1076.
- Rodrigues, H., Jacobs, C., Guedes, J., Bendsøe, M., 1999. Global and local material optimization applied to anisotropic bone adaptation. In: Perdersen, P., Bendsoe, M.P. (Eds.), *Synthesis in Bio Solid Mechanics*. Kluwer Academic Publishers, pp. 209–220 ISBN 0-7923-5615-2.
- Santos, L., Coelho, P., Fonseca, J., Rodrigues, H., Fernandes, P., 2008. A DXA validation of a bone remodeling model for the assessment of osteoporotic bone quality. Sixth International Conference on Engineering Computational Technology, M. Papadarakakis and B.H.V. Topping, (Eds.), Civil-Comp Press, Stirling-shire, Scotland.
- Sigmund, O., 1999. On the optimality of bone structure. In: Perdersen, P., Bendsoe, M.P. (Eds.), *Synthesis in Bio Solid Mechanics*. Kluwer Academic Publishers, pp. 221–234 ISBN 0-7923-5615-2.
- Svanberg, K., 1987. The method of moving asymptotes—a new method for structural optimisation. *International Journal for Numerical Methods in Engineering* 24, 359–373.
- Taylor, D., Lee, T.C., 2003. Microdamage and mechanical behavior: predicting failure and remodeling in compact bone. *Journal of Anatomy* 203, 203–211.
- Taylor, D., Casolari, E., Bignardi, C., 2004. Predicting stress fractures using a probabilistic model of damage, repair and adaptation. *Journal of Orthopaedic Research* 22, 487–494.
- Viceconti, M., Casali, M., Massari, B., Cristofolini, L., Bassini, S., Toni, A., 1996. The 'standardized femur program' proposal for a reference geometry to be used for the creation of finite element models of the femur. *Journal of Biomechanics* 29, 1241.
- Weinans, H., Huiskes, R., Grootenboer, H.J., 1992. The behavior of adaptive bone-remodeling simulation models. *Journal of Biomechanics* 25, 1425–1441.
- Wolff, J., 1986. *The law of bone remodeling (Das Gesetz der Transformation der Knochen, Hirschwald, 1892)*. Translated by Maquet P. and Furlong R. Springer, Berlin.